Proton-coupled electron transfer mechanisms of the copper centres of nitrous oxide reductase from *Marinobacter hydrocarbonoclasticus* – an electrochemical study

Cíntia Carreira[1,2], Margarida M. C. dos Santos[3], Sofia R. Pauleta[1*], Isabel Moura[2*]

[1] Microbial Stress Lab, UCIBIO, REQUIMTE, Departamento de Química, Faculdade de Ciências e Tecnologia, Universidade Nova de Lisboa, Campus da Caparica, 2829-516 Caparica, Portugal.

[2] Biological Chemistry Lab, LAQV, REQUIMTE, Departamento de Química, Faculdade de Ciências e Tecnologia, Universidade Nova de Lisboa, Campus da Caparica, 2829-516 Caparica, Portugal.

[3] Centro de Química Estrutural, Instituto Superior Técnico, Universidade de Lisboa, Av. Rovisco Pais, 1049-001 Lisboa, Portugal.

***Corresponding Authors**

Sofia R. Pauleta

Microbial Stress Lab, UCIBIO, REQUIMTE, Departamento de Química, Faculdade de Ciências e Tecnologia, Universidade Nova de Lisboa, Campus da Caparica, 2829-516 Caparica, Portugal. Email: srp@fct.unl.pt

Tel. +351 212 948 385, ext. 10967

Fax: + 351 212 948 550

http://docentes.fct.unl.pt/srp/

Isabel Moura

Biological Chemistry Lab, LAQV, REQUIMTE, Departamento de Química, Faculdade de Ciências e Tecnologia, Universidade Nova de Lisboa, Campus da Caparica, 2829-516 Caparica, Portugal. Email: isabelmoura@fct.unl.pt

Tel. +351 212 948 385, ext. 10916

Fax: + 351 212 948 550

Abstract

Reduction of N_2O to N_2 is catalysed by nitrous oxide reductase in the last step of the denitrification pathway. This multicopper enzyme has an electron transferring centre, CuA, and a tetranuclear copper-sulfide catalytic centre, "CuZ", which exists as CuZ*(4Cu1S) or CuZ(4Cu2S). The redox behaviour of these metal centres in *Marinobacter hydrocarbonoclasticus* nitrous oxide reductase was investigated by potentiometry and for the first time by direct electrochemistry. The reduction potential of CuA and CuZ(4Cu2S) was estimated by potentiometry to be +275±5 mV and +65±5 mV *vs* SHE, respectively, at pH 7.6. A proton-coupled electron transfer mechanism governs CuZ(4Cu2S) reduction potential, due to the protonation/deprotonation of Lys397 with a pK_{ox} of 6.0±0.1 and a pK_{red} of 9.2±0.1. The reduction potential of CuA, in enzyme samples with CuZ*(4Cu1S), is controlled by protonation of the coordinating histidine residues in a two-proton coupled electron transfer process. In the cyclic voltammograms, two redox pairs were identified corresponding to CuA and CuZ(4Cu2S), with no additional signals being detected that could be attributed to CuZ*(4Cu1S). However, an enhanced cathodic signal for the activated enzyme was observed under turnover conditions, which is explained by the binding of nitrous oxide to CuZ^0(4Cu1S), an intermediate species in the catalytic cycle.

Keywords: Nitrous oxide reductase, direct electrochemistry, CuA centre, CuZ centre, proton-coupled electron transfer, potentiometry

1. Introduction

Nitrous oxide (N_2O) is a potent greenhouse gas and an ozone depleting agent whose emission to the atmosphere has been enhanced in the last century through anthropogenic activities, especially with the large use of synthetic fertilizers in agriculture [1, 2]. Removal of this gas from the atmosphere is challenging and in nature, only some archaea, soil and marine bacteria have been found to have encoded in their genome an enzyme, named nitrous oxide reductase (N_2OR), able to reduce N_2O during anoxic or microoxic respiration [3]. N_2OR is a copper dependent enzyme that catalyses the last step of the denitrification pathway: the two-proton and two-electron reduction of N_2O to the inert dinitrogen gas and water [4] (Eq. 1).

$$N_2O + 2\ e^- + 2\ H^+ \leftrightarrow N_2 + H_2O \quad E^{o\prime} = 1.35\ V,\ pH\ 7.0 \quad (1)$$

N_2OR is a functional homodimeric enzyme that has been divided in two different classes. Clade I N_2OR contains two multicopper redox centres, CuA, the electron transferring centre and "CuZ" centre, the catalytic centre, that has an affinity for N_2O of around 20 μM [5]. On the other hand, clade II N_2OR has a higher substrate affinity [6], but with lower maximum rate of reaction, and besides the two structural domains (the CuA binding cupredoxin-domain and the "CuZ" binding β-propeller domain) has, in some cases, an additional *c*-type haem in an additional C-terminal domain [7].

CuA centre is a mixed-valence binuclear copper centre well-characterized and similar to the one found in cytochrome *c* oxidase [8-10]. This redox active centre exhibits absorption bands at 480, 540 and 800 nm in the [$1Cu^{1.5+}$-$1Cu^{1.5+}$] oxidation state, while in the reduced state it is spectroscopically silent. A reduction potential of + 260 mV *vs* standard hydrogen electrode (SHE) at pH 7.5 was estimated for this redox couple in *Pseudomonas stutzeri* N_2OR [11] and *Paracoccus pantotrophus* N_2OR [12], and a value of 240 mV *vs* SHE at pH 7.6 was estimated for CuA centre in *Marinobacter hydrocarbonoclasticus* N_2OR [13] (Table 1). A similar value was found for the reduction potential of this centre in cytochrome *c* oxidase from *Paracoccus denitrificans* (288 mV) [14] and from *Thermus thermophilus* (250 mV, pH 8.1) [15].

- Insert Table 1 here -

"CuZ" is a tetranuclear copper centre with a central sulfide, unique in biology. Each copper atom of "CuZ" centre is coordinated by two histidine residues with exception of Cu_{IV} that has only one but binds a solvent-derivative molecule or a sulfur atom, which is also shared with Cu_I (Figure 1) [16, 17]. The spectroscopic and structural differences at the Cu_I-Cu_{IV} edge ligand led to the distinction of two types of "CuZ": CuZ*(4Cu1S) and CuZ(4Cu2S). CuZ(4Cu2S), which exhibits an absorption band at 545 nm in the fully oxidized state [$2Cu^{2+}$-$2Cu^{1+}$], can be reduced

to the [$1Cu^{2+}$-$3Cu^{1+}$] oxidation state, which presents an absorption band at 660 nm [18, 19]. The reduction potential of the [$2Cu^{2+}$-$2Cu^{1+}$]/[$1Cu^{2+}$-$3Cu^{1+}$] redox couple was estimated to be + 60 mV *vs* SHE at pH 7.5, in *P. pantotrophus* N_2OR determined in an oxidative potentiometric titration [12] (Table 1). On the other hand, CuZ*(4Cu1S) is a redox inert centre characterized by an absorption band at 640 nm in the [$1Cu^{2+}$-$3Cu^{1+}$] oxidation state and so far its reduction to the [$4Cu^{1+}$] oxidation state has only been observed after prolonged exposure of the enzyme to reduced methyl viologen [20, 21], making its redox properties still an imminent challenge (Table 1).

- Insert Figure 1 here -

The redox properties of CuA and "CuZ" centres will be explored in this work by potentiometry and dynamic electrochemistry.

The dynamic electrochemistry of redox proteins is now an established area of research supported by both fundamental advances in the understanding of long-range electron transfer and the development of new strategies to attain a successful interaction between proteins and electrode surfaces [22]. Nevertheless, for large enzymes, the localization of the redox active centres buried below the protein surface and partial denaturation of the protein on the working electrode may hinder or forbid direct electron transfer. Consequently, there are few reports of direct electrochemical responses of enzymes and in most situations non-catalytic signals are not observed at all, though catalytic signals developed in the presence of substrate are sometimes reported [23, 24]. Alternatively, electron transfer with the electrode can be assisted by a redox mediator, either an artificial or a physiological partner of the enzyme.

Several *c*-type cytochromes have been identified as probable redox partners of clade I N_2ORs isolated from *P. denitrificans* [25, 26], *Rhodobacter capsulatus* [27], *Rhodobacter sphaeroides* [28]*, M. hydrocarbonoclasticus* [29] and also for clade II N_2OR from *Wolinella succinogenes* [30]. Additionally, type 1 copper proteins, namely pseudoazurins, have also been pinpointed as good candidates for the electron transfer to clade I N_2OR from *P. pantotrophus* and *Achromobacter cycloclastes* [31, 32]. However, only the mediated electrocatalysis involving activated *M. hydrocarbonoclasticus* N_2OR and its putative physiological electron donor, cytochrome c_{552} has been investigated [13]. In that study, using a membrane pyrolytic graphite electrode, the rate constant of the intermolecular electron transfer between the two proteins was estimated to be $(5.5 \pm 0.9) \times 10^{-5}$ M^{-1} s^{-1}, in agreement with the values determined for other

electron transfer complexes [33], but no catalytic activity was observed when using the as-isolated *M. hydrocarbonoclasticus* N_2OR. In another study, *A. cycloclastes* pseudoazurin proved to be able to donate electrons to the as-isolated *A. cycloclastes* N_2OR coupled to N_2O reduction, using as working electrode a 4,4-dithiodipyridine-modified gold electrode [32]. In the case of clade II N_2OR from *W. succinogenes* [7], the electron transfer is proposed to occur through the *c*-type haem (in the additional domain) *via* CuA to "CuZ". In this enzyme, no activation seems to be required and direct electron transfer from a glassy carbon electrode through the catalytic centre was reported as a N_2O biosensing system [34].

Up to date, the direct electrochemistry of a clade I N_2OR has never been reported. In this work, the first direct electrochemical response under non-turnover and turnover conditions of clade I *M. hydrocarbonoclasticus* N_2OR is presented. The redox properties of the enzyme were analysed by cyclic voltammetry with the enzyme confined to the surface of a multiwalled carbon nanotubes modified glassy carbon electrode (MWCNT-GCE). Experiments were performed with enzyme samples havong different amounts of CuZ(4Cu2S). Since N_2OR has a very important role in Nature in the N_2O detoxification, studies were also conducted in the presence of substrate with the observation of a signal associated with its catalytic reduction. Such signal is discussed in light of the complex mechanism of activation and catalysis of this enzyme. Additionally, the pH dependence on the reduction potential of CuA and CuZ(4Cu2S) is reported here for the first time.

2. Materials and Methods

2.1 Chemicals and solutions

All chemicals were pro-analysis grade purchased from Merck, Sigma, Panreac, Riedel-de-Haën and Fluka, and used without further purification. All solutions for protein purification were prepared in deionized water and pre-filtered. Solutions for enzymatic assays, potentiometric and voltammetric studies were prepared with Milli-Q water (18.2 MΩ cm, 25 °C). N_2O solution (25 mM at 25 °C) was obtained through saturation of 5 mL of Milli-Q water, trapped in a gas-tight vial (previously degassed with argon) using a gas stock mixture of 5 % Ar/ 95 % N_2O (Air liquid) [35].

All experiments and activation of N_2OR were performed inside an anaerobic chamber (MBraun) at 20 ± 2 ºC, with the O_2 < 4 ppm. Throughout the manuscript, all reduction potential values are referred to the standard hydrogen electrode (SHE) and are affected by an error of 5-10 mV. Experiments were performed at least in duplicate.

2.2 Protein purification and estimation of CuZ(4Cu2S) vs CuZ(4Cu1S)*

N_2OR was isolated from *M. hydrocarbonoclasticus* 617 under oxic or anoxic conditions with "CuZ" centre mainly as CuZ*(4Cu1S) or as CuZ(4Cu2S), respectively as described by *Carreira C.* [36]. Concentration of the monomeric enzyme was determined based on the extinction coefficients previously determined for the dithionite reduced spectrum of N_2OR mainly with CuZ*(4Cu1S) (3500 M^{-1} cm^{-1} at 640 nm [37]) or with CuZ(4Cu2S) (4000 M^{-1} cm^{-1} at 660 nm [36]).

The amount of CuZ(4Cu2S) in each N_2OR preparation was estimated based on the specific activity after 3-5 h reduction in the presence of reduced methyl viologen, assuming that a specific activity of ~200 $\mu mol_{N2O}.min^{-1}.mg^{-1}$ corresponds to a N_2OR preparation with 100 % of CuZ*(4Cu1S) [38]. These activity assays were performed inside a MBraun anaerobic chamber using methyl viologen as the electron donor, as described in [29].

2.3 Potentiometric redox titrations

Potentiometric redox titrations of N_2OR, with 85 % CuZ(4Cu2S), were performed under argon atmosphere in a MBraun anaerobic chamber at 20 ± 2 ºC, by measuring the absorption changes of 60 μM of fully oxidized N_2OR in 100 mM Tris-HCl, pH 7.6 and 2 μM of each mediator (reduction potentials at pH 7.0 [39]: 2,3,5,6-tetramethyl phenylenediamine, + 260 mV; 1,2-naphthoquinone-4-sulfonic acid, 210 mV; 1,2-naphthoquinone, + 180 mV; phenazine

methosulphate, + 80 mV; resorufin, + 65 mV; indigo carmine, - 130 mV; 2-hydroxyl-1,4-naphthoquinone, - 145 mV; methyl viologen, - 430 mV). Throughout the titration, the reduction potential was monitored using a Pt pin electrode combined with an Ag/AgCl reference electrode (Crison). The reduction potential relative to SHE, was obtained by adding 208 mV to the measured value. Small volumes of sodium ascorbate and sodium dithionite (0.1-100 mM) were added with a 10 μL Hamilton syringe in the reductive titration, and potassium ferricyanide (0.1-100 mM) was used for the oxidative titration. For each reduction potential, a spectrum was acquired from 400 nm to 900 nm, using a TIDAS diode array spectrophotometer connected to an external computer. The absorbance at 660 nm and 790 nm was used to follow the reduction/oxidation events related to CuZ(4Cu2S) and CuA centres, respectively. The [oxidized]/[reduced] protein ratio was calculated and plotted as a function of the measured reduction potential. The reduction potentials were obtained from the simulation of the titration curves based on the Nernst equation of one independent reduction for each redox centre.

The evaluation of the pH dependence of the reduction potentials of CuA and "CuZ" centres was performed by potentiometric titrations using the same protein batch or batches with similar percentage of CuZ(4Cu2S) in 100 mM buffer solutions of MES (pH 5.5-6.5), HEPES (pH 7.0), Tris-HCl (pH 7.6-8.5) and CHES (pH 9.0-9.5). The pH value of the solution was checked at the end of each potentiometric titration.

2.4 Direct electrochemical measurements

Direct electrochemical measurements by cyclic voltammetry of N_2OR with 65% and 40% of CuZ(4Cu2S) were conducted inside the anaerobic chamber. The CV experiments were performed with an EcoChemie μAutolab potentiostat/galvanostat (Metrohm Autolab, The Netherlands). Parameters of the equipment and data acquisition were controlled with GPES v. 4.9 software also from EcoChemie.

In typical experiments the cyclic voltammograms (CVs) were obtained in the potential range between + 0.9 and - 0.5 V *vs* SHE and the scan rate (v) varied between 5 and 100 mV s^{-1}.

A conventional three-electrode configuration cell was used with a platinum wire auxiliary electrode and an Ag/AgCl reference electrode (+ 208 mV *vs* SHE) (BAS ref. MF-2052). The working electrode was a multiwalled carbon nanotubes (MWCNT) modified glassy carbon electrode (GCE - BAS ref. MF2012).

2.4.1 Preparation of the MWCNT modified GCE

MWCNT (Sigma) were functionalized in 3 M HNO_3 during 24 h, as described in [40]. MWCNT were then washed with Milli-Q water in a paper filter until the discarded water reached a pH ~7.0. A thermal treatment of MWCNTs was performed at 80 °C for 24 h followed by its dispersion into 1 % w/v dimethylformamide and sonication for 3 h.

Before each experiment, GCE was polished with 1 and 0.5 μm alumina slurry, sonicated for 5 minutes and rinsed with deionized water. Functionalized 7 μL MWCNT were deposited on the electrode surface and left to dry for 45 min, at room temperature. A drop of 10 μL N_2OR solution was applied on the surface of MWCNT and left to dry for 45 min before electrode immersion in the electrolyte solution.

2.4.2 Electrolyte

In typical experiments, the supporting electrolyte was 100 mM potassium phosphate buffer at pH 7.0.

2.4.3 Catalytic turnover

Turnover assays were conducted using activated N_2OR with 40 and 65 % of CuZ(4Cu2S). Activated enzyme (after 3 h incubation with reduced methyl viologen in 100 mM Tris-HCl pH 7.6, inside an anaerobic chamber) was desalted using a NAP-5 Sephadex G25 column (GE Healthcare) equilibrated with 100 mM potassium phosphate pH 7.0 [29]. The collected enzyme was concentrated using an ultrafiltration micro concentrator (MW cut off 30 kDa) to a final concentration of 124 μM. A drop of this activated N_2OR (4 μL) was immobilized on the MWCNT-GCE, using the procedure described before. Turnover assays were also performed in 100 mM potassium phosphate pH 7.0 electrolyte solution, in the presence of increasing concentrations of N_2O-saturated water, up to 1.4 mM.

3. Results

3.1 pH dependence of the reduction potential of M. hydrocarbonoclasticus N_2OR redox centres by potentiometry

Spectroscopic studies showed that both CuA and CuZ(4Cu2S) centres from *M. hydrocarbonoclasticus* N_2OR can be reversibly reduced, contrary to CuZ*(4Cu1S) centre, which can only be reduced after a prolonged incubation in the presence of reduced methyl viologen [41].

The potentiometric titrations show that CuA and CuZ(4Cu2S) centres behave independently in an oxidation/reduction process and a one-electron reduction is associated to each centre, according to the slope of the fitted curves (Figure 2). A similar behaviour was reported for CuA and CuZ(4Cu2S) centres of *M. hydrocarbonoclasticus* and *P. pantotrophus* N_2ORs, respectively [12, 13].

The oxidative and reductive titration curves at pH 7.6 show no evidence of hysteresis (Figure 2). The variation of the absorbance at 790 nm and 660 nm with the reduction potential was fitted to the Nernst equation and reduction potentials of + 275 ± 5 mV and + 65 ± 5 mV *vs* SHE, were estimated at pH 7.6, respectively, for a sample containing 85% of CuZ(4Cu2S). The more positive reduction potential is assigned to the $[1Cu^{1.5+}\text{-}1Cu^{1.5+}]/[1Cu^{1+}\text{-}1Cu^{1+}]$ redox couple of CuA centre, and is similar to the value previously reported (+ 240 mV at pH 7.6, for a N_2OR preparation containing 35 % of CuZ(4Cu2S) [13]). The lower reduction potential corresponds to the $[2Cu^{2+}\text{-}2Cu^{1+}]/[1Cu^{2+}\text{-}3Cu^{1+}]$ redox couple of CuZ(4Cu2S) centre, in agreement with the value determined for this centre in an oxidative titration of *P. pantotrophus* N_2OR (+ 60 mV at pH 7.5, determined for an enzyme preparation with 65 % of CuZ(4Cu2S)) [12].

- Insert Figure 2 here -

Potentiometric studies were also conducted to investigate the pH dependence of CuA and CuZ(4Cu2S) reduction potential (Table 2).

The pH profile of the reduction potential of CuA centre depends on the percentage of CuZ(4Cu2S) in the enzyme preparation used in the potentiometric titrations (Figure 3 and Table 2), but no hysteresis is observed (see Figure S1 in Supplementary Material). The reduction potential of CuA centre in N_2OR with a high percentage of CuZ(4Cu2S) almost does not change in the pH range studied (Figure 3B and Table 2), while in enzyme preparations with a lower content of CuZ(4Cu2S) the reduction potential varied linearly with pH, with a slope of - 54 mV

per pH unit (Figure 3A and Table 2). Although this value could be considered close to the expected - 58 mV per pH unit, for a H^+/e^- coupled process at 20 °C, taking into account the percentage of CuZ(4Cu2S) of the enzyme preparations used, a different interpretation can be made. As described in Supplementary Material S1, the reduction potential of CuA centre can be estimated for a N_2OR sample with either 0% of CuZ(4Cu2S) or 100 % CuZ(4Cu2S) (Figure 3C and Table S1 in Supplementary Material S1). This analysis clearly shows that the reduction potential of CuA in a sample with 100% of CuZ(4Cu2S) does not change in the pH range studied, while in enzyme preparations with 0% of CuZ(4Cu2S), it varies linearly with a slope of – 110 mV per pH unit, which indicates the presence of a $2H^+/e^-$ coupled process (Figure 3C).

- Insert Figure 3 here -

For "CuZ" centre, the potentiometric titrations performed at pH 6.5 and 9.0 showed a significative hysteresis between the oxidative and the reductive titration (Figure 4, Table 2), which is a redox behaviour different from the one observed at pH 7.6 (Figure 2). The hysteresis has a difference of about 60 mV and is explained by the reductive titration having a pH dependence (*vide infra*). In fact, the reduction potential of the reductive titration depends on pH (- 55 mV per pH unit) (see Figure 4C), which is consistent with a redox process coupled with proton binding [39], suggesting that the one-electron reduction of CuZ(4Cu2S) is associated with the binding of one proton. In the oxidative titration, the reduction potential does not vary significantly among the pH values tested, suggesting a non-pH dependence of the reduction potential during oxidation.

- Insert Figure 4 here -

- Insert Table 2 here -

3.2 Direct electrochemistry under non-turnover conditions

The direct electrochemistry of *M. hydrocarbonoclasticus* N_2OR was investigated by cyclic voltammetry at different electrodes with the enzyme either immobilized at the electrode surface or entrapped by a dialysis membrane.

In the case of carbon electrodes, neomycin was used as co-absorbant, being added to the protein solution and to the electrolyte medium to improve the interaction between *M.*

hydrocarbonoclasticus N_2OR (pI=5.4 [37]) and the electrode, as both surfaces are negatively charged at pH 7.0. Gold electrodes, bare and modified with dipyridyl, neomycin and polylysine, were also tested. In all situations no electrochemical signals, distinguishable from the CVs of the electrolyte solution, were observed with the enzyme as a film on the electrode surface, in solution or confined by a membrane as a thin layer near the electrode surface.

A direct electrochemical response of *M. hydrocarbonoclasticus* N_2OR, with 40 % of CuZ(4Cu2S), was achieved when the enzyme was immobilized on a glassy carbon electrode (GCE) coated with a multiwalled carbon nanotubes (MWCNT). The modification of GCE was monitored through the analysis of the CVs of the electrolyte solution that revealed enhanced but reproducible capacitive background currents, indicating that this was an efficient process. A ratio of the electroactive area, A_{ele}, to the geometric area, A_{geo}, was estimated to be ~110, from the values of the capacitive current obtained at the MWCNT-GCE and bare GCE.

In Figure 5 are shown the CVs obtained at the MWCNT-GCE before (dashed line) and after protein immobilization (solid line). Well-defined redox peaks were obtained for the protein confined to the electrode surface. The CV revealed the presence of two redox pairs: signal I, with a cathodic peak (Ep_c^I) and an anodic counterpart (Ep_a^I) and signal II with a second cathodic peak (Ep_c^{II}) at more negative potentials, and a less clear anodic counterpart (Ep_a^{II}). This behaviour was observed for the as-isolated and activated N_2OR, independently of the percentage of CuZ(4Cu2S) present in the N_2OR preparations (data not shown).

- Insert Figure 5 here –

The behaviour of N_2OR on the MWCNT-GCE was investigated by varying the scan rate, v, in the range of 5 to 100 mV s^{-1} (Figure 6A).

The redox process associated with signal I deviates from reversibility with increasing v, since the separation between the peak potentials, ΔE_p, increases [42], varying from 40 mV at 5 mV s^{-1} to 308 mV at 100 mV s^{-1}. As to the peak currents, the ratio (I_{pa}^I / I_{pc}^I) is close to 1, independently of the scan rate. Two different behaviours of the peak currents with v were detected: in between 5 and 50 mV s^{-1}, a linear relation of the peak currents with v was observed in accordance with a diffusion-less process, while for v >50 mV s^{-1} a negative deviation of the linearity of the peak currents was observed due to the deviation from reversibility of the redox process (Figure 6B). The average of the anodic and cathodic peak potentials of signal I, ($Ep_c^I + Ep_a^I$)/2, remains constant and therefore a reduction potential, $E°'^I$, at pH 7.0 was estimated to be + 385 ± 10 mV

(*vs* SHE) [42]. Additionally, signal I corresponds to a one-electron transfer reaction, given that the width at half-height ($\Delta E_{p,1/2}$) has a value of 100 mV, close to the theoretical value of 90 mV for a reversible one-electron diffusion less redox process [42]. Taking into consideration the reduction potential determined for signal I, this signal is assigned to CuA centre of N_2OR as this centre is the one with the more positive reduction potential (Table 2).

- Insert Figure 6 here -

As to signal II, it is noticeable a second cathodic peak (Ep_c^{II}) at more negative potentials with an anodic counterpart, (Ep_a^{II}) best observed at low scan rates ($\leq$ 20 mV s^{-1}) (Figure 6A). The redox process associate with signal II is not reversible, as there is a linear variation of the cathodic potential, Ep_c^{II} with the logarithm of the scan rate, for scan rates > 20 mV s^{-1} (Figure 6C). Therefore, a reduction potential, $E°'^{II}$, of + 70 ± 10 mV (*vs* SHE) at pH 7.0, was estimated for signal II, from the average of the cathodic (Ep_c^{II} = + 21 mV) and anodic peak potentials (Ep_a^{II} = + 119 mV), observed for the lowest scan rate used. Signal II is assigned to CuZ(4Cu2S) centre since its reduction potential is lower than the one of CuA centre, and the value estimated by cyclic voltammetry is similar to the one determined by potentiometry at this pH (+ 81 ± 5 mV, Table 2).

3.3 Direct electrochemistry under turnover conditions

The catalytic activity of the as-isolated and activated *M. hydrocarbonoclasticus* N_2OR with 65 or 40 % of CuZ(4Cu2S), was investigated at pH 7.0 in the presence of N_2O.

The CV of as-isolated N_2ORs did not change in the presence of N_2O (data not shown), while after activation an increase in the cathodic peak current around Ep_c^{II} (signal II) for [N_2O] > 200 µM is observed (Figure 7) but the more positive signal (signal I) remains unchanged.

- Insert Figure 7 here -

The variation of i_{cat} (measured at + 40 mV in the cathodic wave) with the concentration of substrate was fitted with the Michaelis-Menten equation with an apparent K_M value of 32 ± 9 µM (Figure 7, inset) for N_2OR with 40% of CuZ(4Cu2S). This parameter cannot be compared with the one determined by steady-state kinetics (14 ± 3 µM) [29], as mass limitations cannot be avoided for low concentrations of nitrous oxide.

A turnover number (k_{cat}) of 2.0 ± 0.3 s^{-1} was calculated from the catalytic current, i_{catmax} and Q, the charge associated with the non-turnover signal, according to the equation $k_{cat} = i_{catmax}/Q$. For N_2OR preparations with 65 % of CuZ(4Cu2S), a lower i_{catmax} (1.1 ± 0.2 μA, data not shown) was estimated, from the cyclic voltammogram of the activated enzyme in the presence of 1.0 mM of nitrous oxide.

4. Discussion

Understanding the catalytic mechanism of N_2OR has been a challenge and a matter of discussion in the last decades [13, 41, 43, 44]. Unveil its complexity requires the understanding of the electron transfer events that occur at the two copper centres, especially at the catalytic "CuZ" centre, under turnover and non-turnover conditions.

Towards this aim, the first direct electrochemical study, using cyclic voltammetry, of N_2OR from clade I is reported here, together with potentiometric titrations at different pH values. For that *M. hydrocarbonoclasticus* N_2OR was successfully immobilized on the surface of a glassy carbon electrode coated with a multiwalled carbon nanotubes, and electrochemical signals corresponding to both copper centres were observed.

N_2OR is isolated with "CuZ" centre with different ratios of CuZ(4Cu2S):CuZ*(4Cu1S) (reported here as percentage of CuZ(4Cu2S)), but since CuZ*(4Cu1S) cannot be reduced, by either sodium ascorbate or sodium dithionite, nor oxidized by potassium ferricyanide, the interpretation of the spectral changes during the potentiometric titrations is simplified as these are attributed to oxidation/reduction events of CuA and CuZ(4Cu2S) centres. Moreover, the reduction of CuZ*(4Cu1S) from the [$1Cu^{2+}$:$3Cu^{1+}$] to the [$4Cu^{1+}$] oxidation state occurs after a prolonged reduction in the presence of reduced viologens, while its oxidation has been observed upon titration with potassium ferricyanide (150 ± 5 mV, pH 7.6, in an oxidative titration) [13], as an irreversible process. This behaviour pinpoints to a thermodynamic effect that could potentially be overcome when using an electrode surface as electron donor and hence the reduction of CuZ(4Cu2S), as well as of CuZ*(4Cu1S), could be expected to be observed by cyclic voltammetry. These hypotheses will be discussed here.

4.1 Reduction potential of CuA and "CuZ" centres

The reduction potential of CuA centre estimated by potentiometry at pH 7.0, + 235 ± 5 mV (85% CuZ(4Cu2S)), is similar to the one established for *P. stutzeri* N_2OR (+ 260 mV, pH 7.5, with a similar percentage of CuZ(4Cu2S)) [11] and *P. pantotrophus* N_2OR (+ 260 mV, pH 7.5, 65% CuZ(4Cu2S)) [12]. In the case of *P. stutzeri* N_2OR, the reduction potential of this centre was not reported to depend on the percentage of CuZ(4Cu2S) present in the sample at pH 7.5 [11].

The reduction potential of *M. hydrocarbonoclasticus* N_2OR CuA centre with 50% of CuZ(4Cu2S) was estimated to be + 271 ± 5 mV at pH 7.0, which is higher than the value obtained previously at pH 7.6 (+ 240 mV, 35% CuZ(4Cu2S) [13]), which indicated the presence

of a proton-coupled electron process (*vide infra*).

In the voltammetric approach, the signal assigned to CuA centre has a reduction potential of + 385 ± 10 mV at pH 7.0 (40% CuZ(4Cu2S)), corresponding to a well-behaved redox process. This behaviour is similar to the one of *Thermus thermophilus* cytochrome *c* oxidase CuA centre, that gave a quasi-reversible diffusion controlled one-electron redox signal at a graphite electrode, with a $E^{0'}$ of + 265 mV at pH 6.5 [45]. The 100 mV increase in the reduction potential observed in the voltammetric studies when compared with the value estimated by potentiometry (240 mV ± 10 mV at pH 7.0 [13]) can be explained by the electrocatalytic effect of the CNTs in shifting the reduction potential to more positive values [46].

The reduction potential of CuZ(4Cu2S) centre was estimated to be + 81 ± 5 mV, at pH 7.0 (+ 65 ± 5 mV, at pH 7.6, Table 2) by potentiometry, which is in all similar to the value determined for *P. pantotrophus* N_2OR at pH 7.5 in an oxidative potentiometric titration, 60 ± 5 mV [12]. Moreover, the CV of N_2OR presented a signal with cathodic and anodic contributions, that has a reduction potential of 70 ± 10 mV at pH 7.0 for the lowest scan rate used, which was assigned to CuZ(4Cu2S).

The absence of other signals besides the one mentioned, even in the CVs of N_2OR preparations with 90 % of CuZ*(4Cu1S) (data not shown), is an indication that CuZ*(4Cu1S) cannot be reduced or oxidized by the electrode configurations tested here. Therefore, different strategies to determine the reduction potential of CuZ*(4Cu1S) are still ongoing, using N_2OR preparations with a high content of CuZ*(4Cu1S).

4.2 pH dependence of CuA and "CuZ" reduction potential

The reduction potential of both copper centres presents a pH dependence interpreted as being governed by a proton coupled electron transfer process. An exception was the CuA reduction potential in N_2OR preparations with 100% CuZ(4Cu2S), which was inferred to be pH-independent in the pH range studied here (Table 2 and Figure 3C).

The pH dependence of the reduction potential of CuA centre in N_2OR preparations with low content of CuZ(4Cu2S) is interpreted as being due to the ionization of the imidazole ring of the two histidine residues that coordinate CuA (His526 and His569), as there are no other ionizable groups in close proximity to CuA. These two residues must have similar pK_{ox}s and pK_{red}s, with the pK_{ox} being lower than 5 and the pK_{red} higher than 10 to explain the profile obtained. In fact, a higher pK_{ox} would be translated into changes in CuA absorption bands, which are not observed between pH 5.5 and 7.6 [47], while pK_{red} cannot be estimated by visible spectroscopy as this

centre has no absorption bands in the [Cu^{1+}:Cu^{1+}] oxidation state.

The pH dependence of the reduction potential of "CuZ" centre between pH 6.0 and 9.0 is reported here for the first time. In the potentiometric titrations, with the exception of pH 7.6, it was observed that there is a hysteresis, with *ca.* 60 mV difference between the reductive and the oxidative titration, which can be explained by a pH dependence of the reductive titration. In fact, the reduction potential of the reductive curve decreases with the increase in pH (see Figure 4C), consistent with an one-electron reduction of CuZ(4Cu2S) being associated with the binding of one proton [39].

The hysteresis and pH profile of CuZ(4Cu2S) reduction potential can be explained considering a model with two macroscopic states (oxidized and reduced) with four possible protonated microstates (P_0, P_0H, P_1 and P_1H), which are differently populated at the different pH values depending on the pK_a of the oxidized and reduced microstate (P_0 and P_1) (see Supplementary Material S2). Spectroscopic studies on CuZ(4Cu2S) identified a different pK_a value for the edge sulfur atom in the two oxidation states [48]. In the reduced state, [$1Cu^{2+}$-$3Cu^{1+}$], this atom has a pK_{red} ~ 11, existing as a thiolate ligand at neutral pH, while in the oxidized state, [$2Cu^{2+}$-$2Cu^{1+}$], its pK_{ox} is 3, and thus edge sulfur atom exists mainly as a sulfide ligand at neutral pH. However, when these values are used in the model, the profiles of the molar ratios of the different microstates do not vary between pH 6.5 and 9.0 (see Supplementary Material S2 and Figure S2), suggesting that the redox behaviour observed cannot be explained by the pK_{ox}/pK_{red} values attributed to the core CuZ(4Cu2S) centre.

The reduction potential of a metal centre can be affected by other factors besides the protonation/deprotonation of residues side chains or atoms directly coordinating the centre, such as its secondary coordination sphere ligands and hydrogen bonding network around the metal centre [49]. Therefore, to explain the experimental data, the X-ray structure of N_2OR with "CuZ" centre as CuZ(4Cu2S) was analysed (PDB ID 3SBQ) to identify the presence of ionizable residues in its vicinity. Besides the histidine side chains that coordinate the copper atoms of "CuZ" centre, there is an ionizable residue, Lys397, which is proposed to stabilize the thiolate edge ligand of CuZ(4Cu2S) [50] and thus can influence the reduction potential of this centre. The pK_a of Lys397 was estimated to be 9.2 [50], and since the thiolate sulfur edge is present in the reduced state of CuZ(4Cu2S), then that value can be considered to be pK_{red}. Using the same mathematic model, a pK_{ox} of 6.0 was estimated by fitting the experimental data (Figure 3C). Taking into consideration these two pKs the molar ratio of the different microstates at the different pH values was recalculated (see Supplementary Material S2 and Figure S3). At pH

7.6, the deprotonated form (P_0) dominates the oxidized state, while the protonated form (P_1H) dominates the reduced state. Therefore, at this pH, the reduction from P_0 to P_1H is coupled with a proton transfer. On the other hand, in the oxidized state, at pH 6.5, there is a mixture of the microstates P_0 and P_0H, while the reduced state is dominated by the protonated form (P_1H). A similar effect is observed at pH 9.0, with a mixture of both microstates in the reduced state, while the oxidized state is dominated by the deprotonated form. The lack of dominance of a microstate on the titrations performed at pH 6.5 and 9.0, in either the oxidized or reduced state, respectively can be responsible for the hysteresis observed in the potentiometric titrations.

4.3 N_2OR signals under turnover conditions

There is only one report of a direct electron transfer between an electrode and N_2OR [34], and contrary to the present study, the enzyme belongs to clade II. Moreover, it is important to point out that clade II N_2OR has an additional C-terminal domain, which is suggested to be crucial for the rapid electron transfer and this enzyme has been reported to not require reductive activation [51, 52].

Therefore, direct electrocatalytic activity of the well-characterized clade I N_2OR, which is reported here for the first time, is more challenging due to the absence of the additional domain and by the requirement of activation. Indeed, a small direct electrocatalytic activity was only detected after activation of *M. hydrocarbonoclasticus* N_2OR through the observation of a small catalytic current. The estimated k_{cat} value of 2.0 ± 0.3 s^{-1} (for a N_2OR sample with 40% CuZ(4Cu2S)) is lower than the k_{cat} value > 200 s^{-1} estimated for CuZ*(4Cu1S), by kinetic studies [13, 47], but higher than 0.6 h^{-1}, determined for CuZ(4Cu2S) [41]. Thus, a fraction of N_2OR with CuZ*(4Cu1S) in the fully reduced state is reacting with the substrate N_2O, as the i_{catmax} attained is proportional to the content of CuZ(4Cu2S) present in the enzyme preparation used in the assays. Moreover, the catalytic wave develops at a potential similar to the one observed for CuZ(4Cu2S).

As it is well established that CuZ(4Cu2S) cannot attain high turnover numbers [41], the catalytic wave can be attributed to an intermediate species involved in the catalytic cycle of N_2OR. In fact, the only intermediate species isolated so far, CuZ^0 (CuZ^0(4Cu1S)), has a high catalytic activity and can be reduced to the [$4Cu^{1+}$] oxidation state by an intramolecular electron transfer from CuA indicating that its reduction potential must be positive [13, 47].

Hence, it is reasonable to attribute the catalytic wave observed in the voltammetric experiments to CuZ^0(4Cu1S) (which was formed from CuZ*(4Cu1S) in the fully reduced state after being

exposed to the substrate). Thus, CuZ^0(4Cu1S) and CuZ(4Cu2S) must have relatively similar reduction potentials and are not distinguishable by cyclic voltammetry under these conditions.

5. Conclusions

This work reports the first direct electrochemical characterization of a clade I N_2OR, together with the first analysis of the pH dependence of CuZ(4Cu2S) reduction potential using potentiometry. In addition, it is shown for the first time that CuA reduction potential has a different pH profile in N_2OR preparations with 0 % or 100 % CuZ(4Cu2S).

The potentiometric studies using N_2OR preparation with different CuZ(4Cu2S) content showed that the reduction of CuA in the presence of 0 % CuZ(4Cu2S) (100% CuZ*(4Cu1S)) is coupled to two protons from the two coordinating histidine residues (His526 and His569). In the case of CuZ(4Cu2S) centre, a hysteresis was observed in the reductive titration, which was explained by the involvement of Lys397 that stabilizes the thiolate edge (between Cu_I and Cu_{IV}) in the reduced form of this centre.

In the voltammetric experiments, two redox couples were clearly identified and assigned to CuA and CuZ(4Cu2S) centres of *M. hydrocarbonoclasticus* N_2OR. Nevertheless, the reduction potential of CuZ*(4Cu1S) was still unattainable using the strategies described here, but further efforts are on-going to study its electrochemical behaviour.

This work also reports the first dynamic electrochemical study of clade I N_2OR under turnover conditions, which showed that higher turnover numbers are only attained after activation of the enzyme. The enhanced catalytic current was observed at a reduction potential that is consistent with the expected CuZ^0(4Cu1S) reduction potential. As mentioned before, this form of "CuZ" centre, a catalytic intermediate species, can be reduced by intramolecular electron transfer from CuA centre when this centre is reduced by either sodium ascorbate [47] or cytochrome c_{552} [13]. Future experiments are being carried out to further explore its electrocatalytic properties.

The studies presented here contribute to a better understanding of the redox chemistry of N_2OR metal centres and specially of "CuZ" centre under turnover and non-turnover conditions.

Acknowledgements

We thank Fundação para a Ciência e Tecnologia (FCT) for the financial support through the project PTDC/BBB-BQB/0129/2014 (IM), and the scholarship SFRH/BD/87898/2012 (CC). This work was supported by the Unidade de Ciências Biomoleculares Aplicadas-UCIBIO and Associate Laboratory for Green Chemistry- LAQV, which are financed by national funds from FCT/MCTES, UID/Multi/04378/2019 and UID/QUI/50006/2019, respectively, and by Centro de Química Estrutural multiannual funding 2020 – 2023, UID/QUI/00100/2013, to MMCS.

Author contribution

CC performed the experiments and analysed the data. SRP and MMCS have designed and supervised the experiments and data analysis. IM has designed the experiments and critically revised the manuscript. SRP analysed the date and wrote the paper with contribution from CC, IM and MMCS.

References

[1] A.J. Thomson, G. Giannopoulos, J. Pretty, E.M. Baggs, D.J. Richardson, Biological sources and sinks of nitrous oxide and strategies to mitigate emissions, Philos. Trans. R. Soc. Lond. B Biol. Sci., 367 (2012) 1157-1168.

[2] IPCC 2007 Working group I: the physical science basis, in: S. Solomon, D. Qin, M. Manning, Z. Chen, M. Marquis, K. B. Averyt, M. Tignor, H.L. Miler (Eds.) IPCC - Fourth assessment report: climate change, Cambridge University Press, Cambridge, 2007.

[3] W.G. Zumft, Cell biology and molecular basis of denitrification, Microb. Mol. Biol. Rev., 61 (1997) 533-616.

[4] W.G. Zumft, P.M. Kroneck, Respiratory transformation of nitrous oxide (N_2O) to dinitrogen by Bacteria and Archaea, Adv. Microb. Physiol., 52 (2007) 107-227.

[5] C. Carreira, O. Mestre, R.F. Nunes, I. Moura, S.R. Pauleta, Genomic organization, gene expression and activity profile of *Marinobacter hydrocarbonoclasticus* denitrification enzymes, PeerJ, 6 (2018) e5603.

[6] S. Yoon, S. Nissen, D. Park, R.A. Sanford, F.E. Loffler, Nitrous Oxide Reduction Kinetics Distinguish Bacteria Harboring Clade I NosZ from Those Harboring Clade II NosZ, Appl Environ Microbiol, 82 (2016) 3793-3800.

[7] J. Simon, O. Einsle, P.M. Kroneck, W.G. Zumft, The unprecedented nos gene cluster of *Wolinella succinogenes* encodes a novel respiratory electron transfer pathway to cytochrome *c* nitrous oxide reductase, FEBS Lett., 569 (2004) 7-12.

[8] S. Iwata, C. Ostermeier, B. Ludwig, H. Michel, Structure at 2.8 A resolution of cytochrome *c* oxidase from *Paracoccus denitrificans*, Nature, 376 (1995) 660-669.

[9] T. Tsukihara, H. Aoyama, E. Yamashita, T. Tomizaki, H. Yamaguchi, K. Shinzawa-Itoh, R. Nakashima, R. Yaono, S. Yoshikawa, Structures of metal sites of oxidized bovine heart cytochrome *c* oxidase at 2.8 A, Science, 269 (1995) 1069-1074.

[10] J.M. Charnock, A. Dreusch, H. Körner, F. Neese, J. Nelson, A. Kannt, H. Michel, C.D. Garner, P.M. Kroneck, W.G. Zumft, Structural investigations of the CuA centre of nitrous oxide reductase from *Pseudomonas stutzeri* by site-directed mutagenesis and X-ray absorption spectroscopy, Eur. J. Biochem., 267 (2000) 1368-1381.

[11] C.L. Coyle, W.G. Zumft, P.M. Kroneck, H. Körner, W. Jakob, Nitrous oxide reductase from denitrifying *Pseudomonas perfectomarina*. Purification and properties of a novel multicopper enzyme, Eur. J. Biochem., 153 (1985) 459-467.

[12] T. Rasmussen, B.C. Berks, J.N. Butt, A.J. Thomson, Multiple forms of the catalytic centre, CuZ, in the enzyme nitrous oxide reductase from *Paracoccus pantotrophus*, Biochem. J., 364 (2002) 807-815.

[13] S. Dell'Acqua, S.R. Pauleta, P.M. Paes de Sousa, E. Monzani, L. Casella, J.J. Moura, I. Moura, A new CuZ active form in the catalytic reduction of N_2O by nitrous oxide reductase from *Pseudomonas nautica*, J. Biol. Inorg. Chem., 15 (2010) 967-976.

[14] H. Wang, D.F. Blair, W.R. Ellis, Jr., H.B. Gray, S.I. Chan, Temperature dependence of the reduction potential of CuA in carbon monoxide inhibited cytochrome c oxidase, Biochemistry, 25 (1986) 167-171.

[15] C.E. Slutter, D. Sanders, P. Wittung, B.G. Malmstrom, R. Aasa, J.H. Richards, H.B. Gray, J.A. Fee, Water-soluble, recombinant CuA-domain of the cytochrome ba3 subunit II from Thermus thermophilus, Biochemistry, 35 (1996) 3387-3395.

[16] K. Brown, K. Djinovic-Carugo, T. Haltia, I. Cabrito, M. Saraste, J.J. Moura, I. Moura, M. Tegoni, C. Cambillau, Revisiting the catalytic CuZ cluster of nitrous oxide (N2O) reductase. Evidence of a bridging inorganic sulfur, J. Biol. Chem., 275 (2000) 41133-41136.

[17] A. Pomowski, W.G. Zumft, P.M.H. Kroneck, O. Einsle, N_2O binding at a 4Cu:2S copper-sulphur cluster in nitrous oxide reductase, Nature, 477 (2011) 234-237.

[18] S. Dell'Acqua, S.R. Pauleta, J.J. Moura, I. Moura, Biochemical characterization of the purple form of *Marinobacter hydrocarbonoclasticus* nitrous oxide reductase, Philos. Trans. R. Soc. Lond. B Biol. Sci., 367 (2012) 1204-1212.

[19] S.R. Pauleta, S. Dell'Acqua, I. Moura, Nitrous oxide reductase, Coord. Chem. Rev., 257 (2013) 332-349.

[20] J.M. Chan, J. Bollinger, C.L. Grewell, D.M. Dooley, Reductively activated nitrous oxide reductase reacts directly with substrate, J. Am. Chem. Soc., 126 (2004) 3030-3031.

[21] S. Ghosh, S.I. Gorelsky, P. Chen, I. Cabrito, J.J.G. Moura, I. Moura, E.I. Solomon, Activation of N_2O reduction by the fully reduced mu_4-sulfide bridged tetranuclear CuZ cluster in nitrous oxide reductase, J. Am. Chem. Soc., 125 (2003) 15708-15709.

[22] F.A. Armstrong, Recent developments in dynamic electrochemical studies of adsorbed enzymes and their active sites, Curr. Opin. Chem. Biol., 9 (2005) 110-117.

[23] C. Léger, P. Bertrand, Direct electrochemistry of redox enzymes as a tool for mechanistic studies, Chem. Rev., 108 (2008) 2379-2438.

[24] V. Fourmond, C. Léger, Protein Electrochemistry: Questions and Answers, in: L.J.C. Jeuken (Ed.) Biophotoelectrochemistry: From Bioelectrochemistry to Biophotovoltaics, Springer International Publishing, Cham, 2016, pp. 1-41.

[25] F.C. Boogerd, H.W. van Verseveld, A.H. Stouthamer, Electron transport to nitrous oxide in *Paracoccus denitrificans*, FEBS Lett, 113 (1980) 279-284.

[26] J.W.B. Moir, S.J. Ferguson, Properties of a *Paracoccus denitrificans* mutant deleted in cytochrome c_{550} indicate that a copper protein can substitute for this cytochrome in electron transport to nitrite, nitric oxide and nitrous oxide, Microbiology, 140 (1994) 389-397.

[27] D.J. Richardson, L.C. Bell, A.G. McEwan, J.B. Jackson, S.J. Ferguson, Cytochrome c_2 is essential for electron transfer to nitrous oxide reductase from physiological substrates in

Rhodobacter capsulatus and can act as an electron donor to the reductase in vitro. Correlation with photoinhibition studies, Eur J Biochem, 199 (1991) 677-683.

[28] M. Itoh, K. Matsuura, T. Satoh, Involvement of cytochrome bc1 complex in the electron transfer pathway for N_2O reduction in a photodenitrifier, *Rhodobacter sphaeroides* f. s. *denitrificans*, FEBS Letters, 251 (1989) 104-108.

[29] S. Dell'acqua, S.R. Pauleta, E. Monzani, A.S. Pereira, L. Casella, J.J.G. Moura, I. Moura, Electron transfer complex between nitrous oxide reductase and cytochrome c_{552} from *Pseudomonas nautica*: kinetic, nuclear magnetic resonance, and docking studies, Biochemistry, 47 (2008) 10852-10862.

[30] C.-s. Zhang, T.C. Hollocher, The reaction of reduced cytochromes *c* with nitrous oxide reductase of *Wolinella succinogenes*, Biochimica et Biophysica Acta (BBA) - Bioenergetics, 1142 (1993) 253-261.

[31] T. Rasmussen, T. Brittain, B.C. Berks, J. Watmough, A.J. Thomson, Formation of a cytochrome *c* – nitrous oxide reductase complex is obligatory for N_2O reduction by *Paracoccus pantotrophus*, Dalton Trans., (2005) 3501-3506.

[32] K. Fujita, M. Hirasawa-Fujita, D.E. Brown, Y. Obara, F. Ijima, T. Kohzuma, D.M. Dooley, Direct electron transfer from pseudoazurin to nitrous oxide reductase in catalytic N_2O reduction, J. Inorg. Biochem., 115 (2012) 163-173.

[33] P.M. Paes de Sousa, S.R. Pauleta, M.L. Simões Gonçalves, G.W. Pettigrew, I. Moura, M.M. Correia dos Santos, J.J.G. Moura, Mediated catalysis of *Paracoccus pantotrophus* cytochrome *c* peroxidase by *P. pantotrophus* pseudoazurin: kinetics of intermolecular electron transfer, J. Biol. Inorg. Chem., 12 (2007) 691-698.

[34] W. Tsugawa, H. Shimizu, M. Tatara, Y. Ueno, K. Kojima, K. Sode, Nitrous Oxide Sensing using Oxygen-Insensitive Direct-Electron-Transfer-Type Nitrous Oxide Reductase, Electrochemistry, 80 (2012) 371-374.

[35] J.K. Kristjansson, T.C. Hollocher, First practical assay for soluble nitrous oxide reductase of denitrifying bacteria and a partial kinetic characterization, J. Biol. Chem., 255 (1980) 704-707.

[36] C. Carreira, Insights into the structure and reactivity of the catalytic site of nitrous oxide reductase, Dept. Química, Universidade Nova de Lisboa, Caparica, 2017, pp. 264.

[37] M. Prudêncio, A.S. Pereira, P. Tavares, S. Besson, I. Cabrito, K. Brown, B. Samyn, B. Devreese, J. Van Beeumen, F. Rusnak, G. Fauque, J.J. Moura, M. Tegoni, C. Cambillau, I. Moura, Purification, characterization, and preliminary crystallographic study of copper-containing nitrous oxide reductase from *Pseudomonas nautica* 617, Biochemistry, 39 (2000) 3899-3907.

[38] C. Carreira, S.R. Pauleta, I. Moura, The catalytic cycle of nitrous oxide reductase - The enzyme that catalyzes the last step of denitrification, J. Inorg. Biochem., 177 (2017) 423-434.

[39] P.L. Dutton, Redox potentiometry: determination of midpoint potentials of oxidation-reduction components of biological electron-transfer systems, Methods Enzymol., 54 (1978) 411-435.

[40] R.C. Carvalho, C. Gouveia-Caridade, C.M. Brett, Glassy carbon electrodes modified by multiwalled carbon nanotubes and poly(neutral red): a comparative study of different brands and application to electrocatalytic ascorbate determination, Anal. Bioanal. Chem., 398 (2010) 1675-1685.

[41] E.M. Johnston, S. Dell'Acqua, S. Ramos, S.R. Pauleta, I. Moura, E.I. Solomon, Determination of the active form of the tetranuclear copper sulfur cluster in nitrous oxide reductase, J. Am. Chem. Soc., 136 (2014) 614-617.

[42] A.J. Bard, L.R. Faulkner, Electrochemical Methods, Fundamentals and Applications, Wiley2001.

[43] P. Chen, S.I. Gorelsky, S. Ghosh, E.I. Solomon, N_2O reduction by the mu_4-sulfide-bridged tetranuclear CuZ cluster active site, Angew. Chem. Int. Ed. Engl., 43 (2004) 4132-4140.

[44] S.I. Gorelsky, S. Ghosh, E.I. Solomon, Mechanism of N_2O reduction by the mu_4-S tetranuclear CuZ cluster of nitrous oxide reductase, J. Am. Chem. Soc., 128 (2006) 278-290.

[45] M.K. Ghosh, J. Rajbongshi, D. Basumatary, S. Mazumdar, Role of the surface-exposed leucine 155 in the metal ion binding loop of the CuA domain of cytochrome c oxidase from *Thermus thermophilus* on the function and stability of the protein, Biochemistry, 51 (2012) 2443-2452.

[46] R.C. Carvalho, A. Mandil, K.P. Prathish, A. Amine, C.M.A. Brett, Carbon Nanotube, Carbon Black and Copper Nanoparticle Modified Screen Printed Electrodes for Amino Acid Determination, Electroanalysis, 25 (2013) 903-913.

[47] E.M. Johnston, C. Carreira, S. Dell'Acqua, S. Ghosh, S.R. Pauleta, I. Moura, E.I. Solomon, Spectroscopic Definition of the CuZ^o Intermediate in Turnover of Nitrous Oxide Reductase and Molecular Insight into the Catalytic Mechanism, J. Am. Chem. Soc., 139 (2017) 4462–4476.

[48] E.M. Johnston, S. Dell'Acqua, S.R. Pauleta, I. Moura, E.I. Solomon, Protonation state of the Cu4S2 CuZ site in nitrous oxide reductase: redox dependence and insight into reactivity, Chem. Sci., 6 (2015) 5670-5679.

[49] P. Hosseinzadeh, Y. Lu, Design and fine-tuning redox potentials of metalloproteins involved in electron transfer in bioenergetics, Biochim. Biophys. Acta, 1857 (2016) 557-581.

[50] S. Ghosh, S.I. Gorelsky, S.D. George, J.M. Chan, I. Cabrito, D.M. Dooley, J.J. Moura, I. Moura, E.I. Solomon, Spectroscopic, computational, and kinetic studies of the mu4-sulfide-bridged tetranuclear CuZ cluster in N_2O reductase: pH effect on the edge ligand and its contribution to reactivity, J. Am. Chem. Soc., 129 (2007) 3955-3965.

[51] S. Teraguchi, T.C. Hollocher, Purification and Some Characteristics of a Cytochrome-C-Containing Nitrous-Oxide Reductase from Wolinella-Succinogenes, Journal of Biological Chemistry, 264 (1989) 1972-1979.

[52] S.R. Pauleta, M.S.P. Carepo, I. Moura, Source and reduction of nitrous oxide, Coordination Chemistry Reviews, 387 (2019) 436-449.

[53] S.R. Pauleta, C. Carreira, I. Moura, CHAPTER 7: Insights into Nitrous Oxide Reductase, RSC Metallobiology, 2017, pp. 141-169.

Figures captions

Figure 1 – Structure of "CuZ" centre of nitrous oxide reductase in the (A) CuZ*(4Cu1S) and (B) CuZ(4Cu2S) form, showing the position of the close by lysine residue. Figures were prepared with Biovia Discovery Studio using PDB ID 1QNI for *M. hydrocarbonoclasticus* N_2OR CuZ*(4Cu1S) and PDB ID 3SBP for *P. stutzeri* N_2OR CuZ(4Cu2S). Colour scheme for the atoms: carbon in grey, copper in orange, sulfur in yellow and oxygen in red.

Figure 2 – Potentiometric titration of *M. hydrocarbonoclasticus* N_2OR, with 85 % of CuZ(4Cu2S), performed at pH 7.6 and 20 ºC. (A) The variation in absorbance during oxidation (solid arrow) and reduction (dashed arrow) of N_2OR were followed by visible spectroscopy at 790 nm and 660 nm for CuA and CuZ(4Cu2S) centres, respectively. (B) Reductive (filled symbols) and oxidative (open symbols) titrations for CuA (diamonds) and CuZ(4Cu2S) (circles) centres.

Figure 3 – pH dependence of the reduction potential of CuA centre at 20 ºC. (A) pH dependence of the reduction potential of CuA determined by potentiometry using N_2OR preparations with 50 % of CuZ(4Cu2S). Data obtained has a linear correlation with pH: E(mV) = - 54.5 pH + 654.3, R^2 = 0.992. (B) pH dependence of the reduction potential of CuA determined by potentiometry using N_2OR preparations with 85 % of CuZ(4Cu2S). (C) pH profile of the reduction potential of CuA centre calculated for N_2OR preparations with 0 (open squares) and 100 % of CuZ(4Cu2S) (closed circles) in the pH range studied using Eq. S1 (see Supplementary Material S1). Linear regression E(mV) = -110 pH + 1033.

Figure 4 – pH dependence of the reduction potential of CuZ(4Cu2S) at 20 ºC. Potentiometric titrations of *M. hydrocarbonoclasticus* N_2OR, with 85 % of CuZ(4Cu2S) at pH 6.5 (A) and pH 9.0 (B) were followed at 660 nm in the oxidative (open symbols) and reductive (close symbols) direction. Each titration was fitted to a one-electron process using the Nernst equation with the reduction potentials listed in Table 2. (C) pH dependence of the reductive potentiometric titration. Data were fitted to Equation S2 (see Supplementary Material S2), using a pK_{ox} of 6.0 ± 0.1 and a pK_{red} of 9.2 ± 0.1 and E_{lp} = 160 mV.

Figure 5 – Cyclic voltammogram of *M. hydrocarbonoclasticus* N_2OR with 40 % of CuZ(4Cu2S). 200 μM solution of enzyme in 100 mM potassium phosphate pH 7.0 was

immobilized on the MWCNT-GCE. Dashed line represents the cyclic voltammogram prior to enzyme immobilization and solid line the voltammogram obtained after N_2OR immobilization at a scan rate of 10 mV s^{-1}. The arrow represents the direction of the scan. The cathodic (Ep_c^{I} and Ep_c^{II}) and anodic (Ep_a^{I} and Ep_a^{II}) peak potentials for signal I and signal II are indicated.

Figure 6 – Cyclic voltammograms of *M. hydrocarbonoclasticus* N_2OR with 40 % of CuZ(4Cu2S) at different scan rates. (A) Cyclic voltammograms of 200 μM solution of enzyme, in 100 mM potassium phosphate pH 7.0, immobilized on MWCNT-GCE obtained at $5 \leq \nu \leq 100$ mV s^{-1}. (B) Dependence of signal I anodic (filled symbols) and cathodic (open symbols) peaks currents, I_{pa}^{I} and I_{pc}^{I} with the scan rate. (C) Dependence of signal II cathodic potential, Ep_c^{II}, with the logarithm of the scan rate, for $\nu > 20$ mV s^{-1}.

Figure 7 – Direct electrochemistry of *M. hydrocarbonoclasticus* N_2OR under turnover conditions. Electrocatalytic peak current of 124 μM activated *M. hydrocarbonoclasticus* N_2OR with 40 % of CuZ(4Cu2S) in 100 mM potassium phosphate at pH 7.0 as a function of N_2O added to the electrolyte solution. Data were adjusted to the Michaelis-Menten equation, using K_M of 32 ± 9 μM and i_{catmax} of 2.7 ± 0.2 μA. Inset: cyclic voltammograms of activated N_2OR in the absence of substrate (grey line) and in the presence of 0.45 mM of N_2O-saturated water (solid black line) obtained at the scan rate of 20 mV s^{-1}.

Tables

Table 1 – CuA and "CuZ" centres spectroscopic and redox properties in nitrous oxide reductase.

Center	Visible Absorption[a]		Redox couple	Reduction Potential[b]	Ref.
	Oxidized	Reduced			
CuA	480 nm ($\varepsilon \approx 4000\ M^{-1}cm^{-1}$) 540 nm ($\varepsilon \approx 4000\ M^{-1}cm^{-1}$) 800 nm ($\varepsilon \approx 3000\ M^{-1}cm^{-1}$)	No bands	$[1Cu^{1.5+}:1Cu^{1.5+}]/[1Cu^{1+}:1Cu^{1+}]$	+ (240-260) mV, pH 7.5-7.6	[11, 12]
CuZ (4Cu2S)	545 nm ($\varepsilon \approx 5000\ M^{-1}cm^{-1}$)	660 nm ($\varepsilon \approx 3000$ - 4400 $M^{-1}cm^{-1}$)	$[2Cu^{2+}:2Cu^{1+}]/[1Cu^{2+}:3Cu^{1+}]$	+ 60 mV at pH 7.5	[12, 19, 53]
CuZ* (4Cu1S)	640 nm ($\varepsilon \approx 4000\ M^{-1}cm^{-1}$)	No bands	$[1Cu^{2+}:3Cu^{1+}]/[4Cu^{1+}]$	ND	[19-21, 41]

[a]Molar extinction coefficients, ε, are given by concentration of N_2OR monomer. [b]Reduction potential determined by potentiometric studies. ND – not determined because it is an irreversible process in the conditions tested.

Table 2 – pH dependence of the reduction potential of CuA and CuZ(4Cu2S) centres of *M. hydrocarbonoclasticus* N_2OR.

	N_2OR with 50% CuZ(4Cu2S)	N_2OR with 85% CuZ(4Cu2S)		
	CuA centre	CuA centre	CuZ centre	
pH	$E^{0'}$ (mV)	$E^{0'}$(mV)	$E_{oxidative}$ (mV)	$E_{reductive}$ (mV)
5.5	+ 350	ND	ND	ND
6.0	ND	+ 300	+ 100	+ 140
6.5	+ 312.5	+ 278	+ 66	+ 128
7.0	+ 271	ND	+ 57	+ 105
7.6	+ 240*	+ 275	+ 63	+ 67
8.5	+ 190	ND	ND	ND
9.0	ND	+ 248	+ 60	- 9

Note: * From [13]. ND – not determined. Reduction potential values affected of an error of 5 mV.

Figures

Figure 1

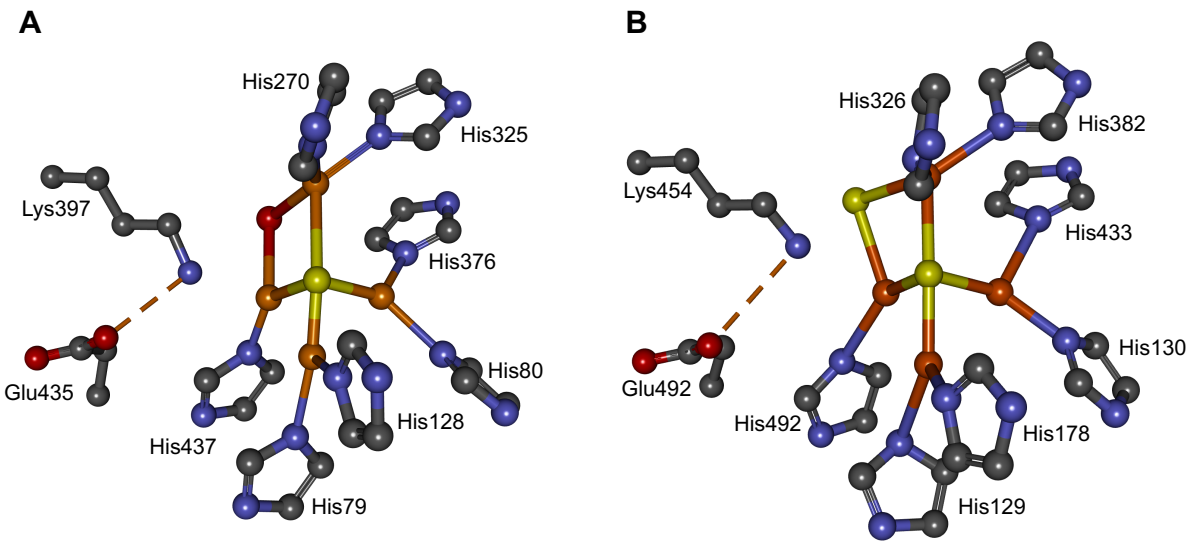

Figure 2

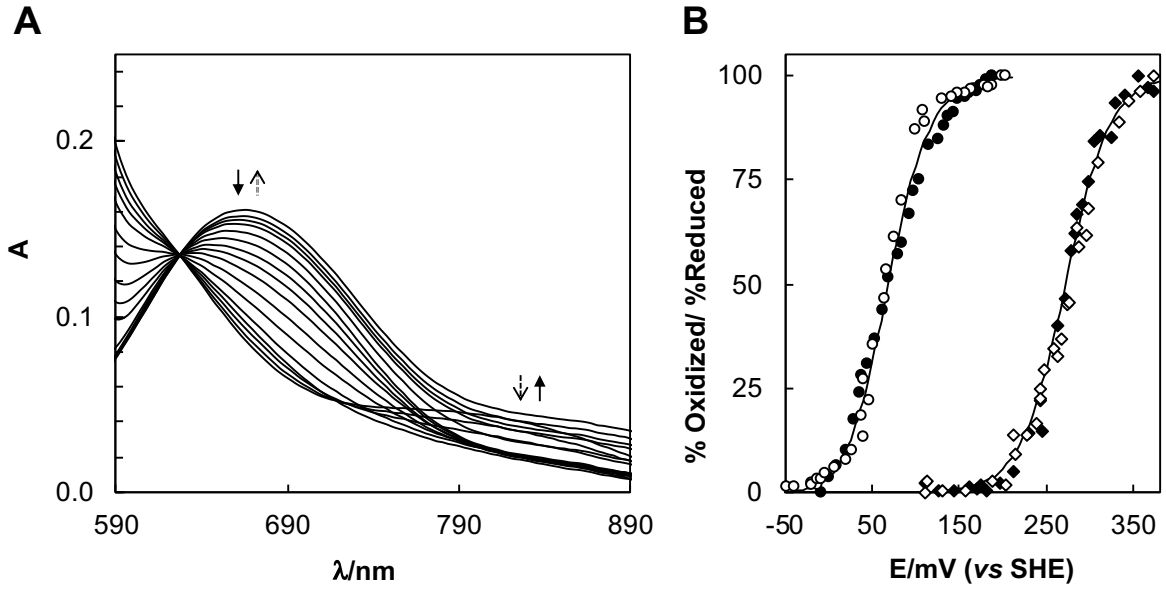
A
0.2
0.1
0.0
A
590
690
790
890
λ/nm
B
100
75
50
25
0
% Oxidized/ %Reduced
-50
50
150
250
350
E/mV (vs SHE)

Figure 3

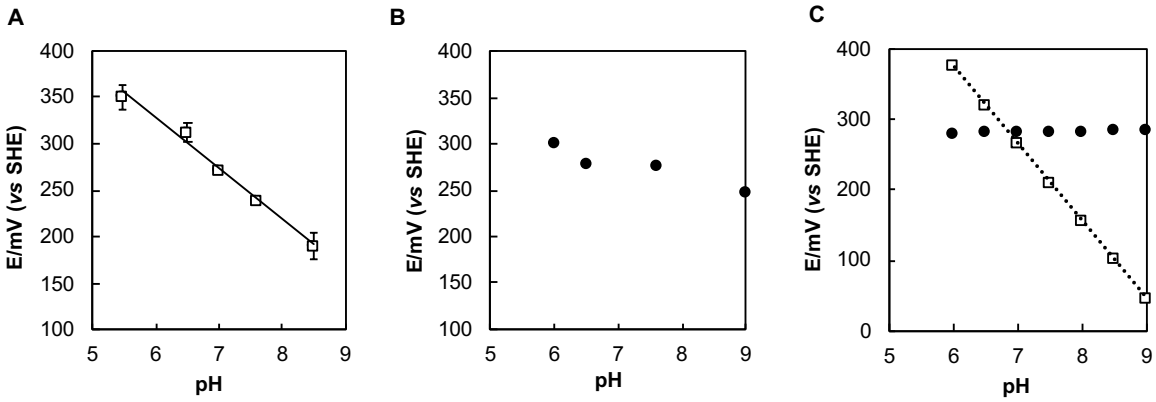

Figure 4

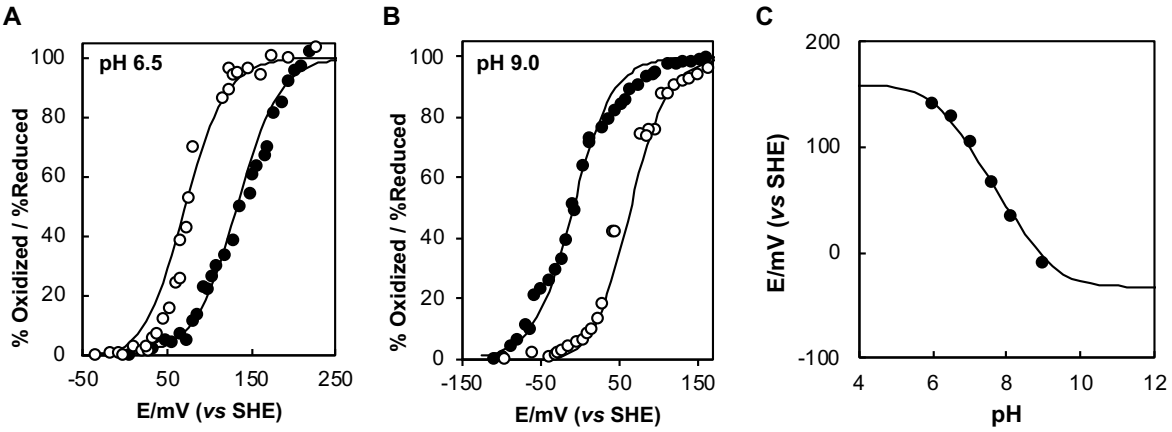
A
pH 6.5
% Oxidized / %Reduced
E/mV (vs SHE)
B
pH 9.0
% Oxidized / %Reduced
E/mV (vs SHE)
C
E/mV (vs SHE)
pH

Figure 5

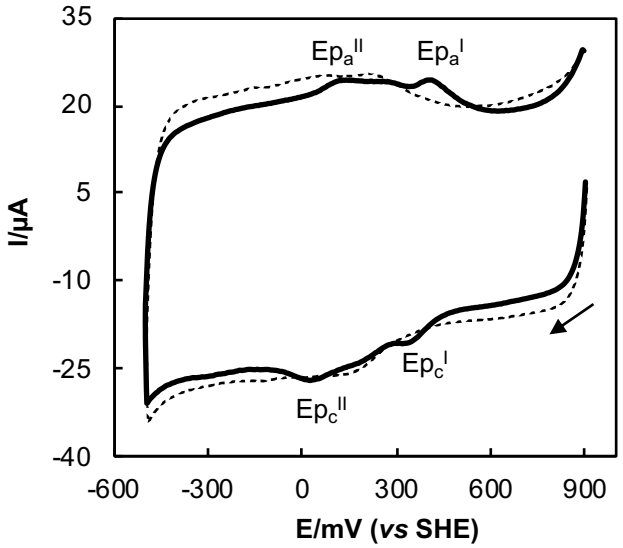
35
20
5
-10
-25
-40
I/µA
-600
-300
0
300
600
900
E/mV (vs SHE)
Epa^II
Epa^I
Epc^I
Epc^II

Figure 6

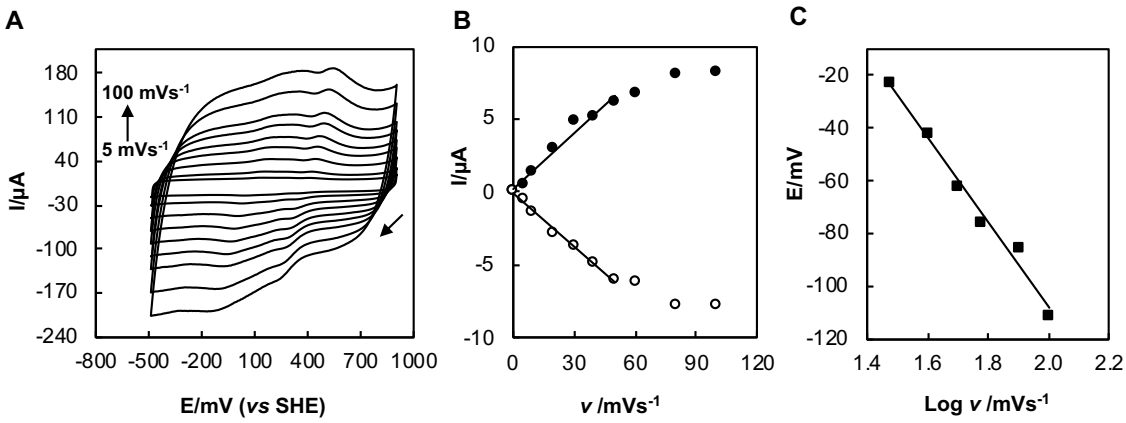

Figure 7

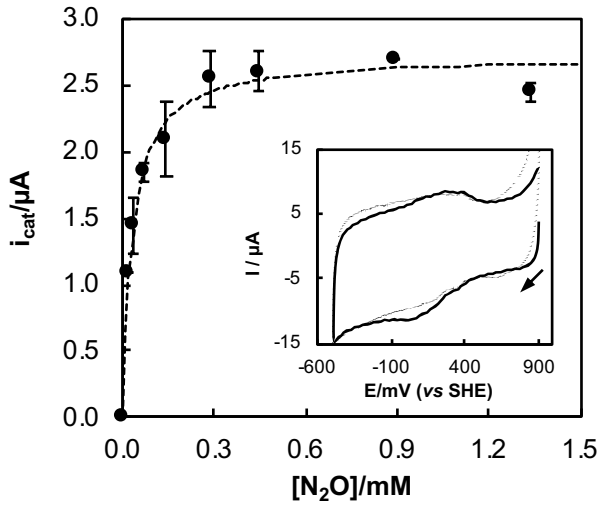
3.0
2.5
2.0
1.5
1.0
0.5
0.0
i_{cat}/μA
0.0
0.3
0.6
0.9
1.2
1.5
[N_2O]/mM
15
5
-5
-15
I / μA
-600
-100
400
900
E/mV (*vs* SHE)